HHS Public Access

Author manuscript

Biol Psychiatry. Author manuscript; available in PMC 2021 July 15.

Published in final edited form as:

Biol Psychiatry. 2020 July 15; 88(2): 139–149. doi:10.1016/j.biopsych.2019.09.018.

Mechanisms underlying the hyperexcitability of CA3 and dentate gyrus hippocampal neurons derived from bipolar disorder patients.

Shani Stern[1,2,*], **Anindita Sarkar**[1], **Tchelet Stern**[1], **Arianna Mei**[1], **Ana P. D. Mendes**[1], **Yam Stern**[1], **Gabriela Goldberg**[1], **Dekel Galor**[1], **Thao Nguyen**[1], **Lynne Randolph-Moore**[1], **Yongsung Kim**[1], **Guy Rouleau**[3], **Anne Bang**[4], **Martin Alda**[5], **Renata Santos**[1,6], **Maria C. Marchetto**[1], **Fred H. Gage**[1,*]

[1]Laboratory of Genetics, Salk Institute for Biological Studies, 10010 North Torrey Pines Road, La Jolla, CA 92037, USA

[2]Sagol Department of Neurobiology, Faculty of Natural Sciences, University of Haifa, Haifa, 3498838, Israel.

[3]Montreal Neurological Institute, McGill University, Montreal

[4]Conrad Prebys Center for Chemical Genomics, Sanford Burnham Prebys Medical Discovery Institute, 10901 North Torrey Pines Road, La Jolla, CA 92037, USA

[5]Department of Psychiatry, Dalhousie University, 5909 Veterans' Memorial Lane, Halifax, NS, B3H 2E2, Canada

[6]Laboratory of Dynamic of Neuronal Structure in Health and Disease, Institute of Psychiatry and Neuroscience of Paris (UMR_S1266 INSERM, University of Paris), 102 rue de la Sante, 75014 Paris, France

Abstract

Background: Approximately one in every 50-100 people is affected with bipolar disorder (BD), making this disease a major economic burden. The introduction of the induced pluripotent stem cells (iPSCs) methodology enabled better modeling of this disorder.

Methods: Having previously studied the phenotype of dentate gyrus (DG) granule neurons, we turned our attention to studying the phenotype of CA3 hippocampal pyramidal neurons of 6 BD patients compared to 4 control individuals. We used patch clamp and qPCR to measure electrophysiological features and RNA expression by specific channel genes.

Results: We found that CA3 BD neurons were hyperexcitable only when they were derived from patients who responded to lithium; they featured sustained activity with large current injections

[*]Co-Corresponding authors: Shani Stern sstern@salk.edu, Fred H. Gage, gage@salk.edu.

Financial disclosures: The authors declare no biomedical financial interests or potential conflicts of interest.

and a large, fast after-hyperpolarization, similar to what we previously reported in DG neurons. The higher amplitudes and faster kinetics of fast potassium currents correlated with this hyperexcitability. Further supporting the involvement of potassium currents, we observed an overexpression of Kcnc1 and Kcnc2 in hippocampal neurons derived from lithium responders. Applying specific potassium channel blockers diminished the hyperexcitability. Chronic lithium treatment decreased the hyperexcitability observed in the CA3 neurons derived from lithium responders, while increasing sodium currents and reducing fast potassium currents. When differentiating this cohort into spinal motor neurons, we did not observe any changes in the excitability of BD motor neurons compared to control motor neurons.

Conclusions: The hyperexcitability of BD neurons is neuronal type specific with the involvement of altered potassium currents that allow for a sustained, continued firing activity.

Keywords

Bipolar disorder; hippocampus; dentate gyrus; pyramidal; hyperexcitability; motor neurons

Introduction

Bipolar disorder (BD) affects around 1-2.5% of the worldwide population, with different severity in the symptoms (1-3). People with this disorder suffer from episodes of mania. Lithium remains among the first-line treatments for both acute episodes and long-term prevention of manic and depressive recurrences. BD has a complex genetic background; many genes are known to associate with it (4-6) but each gene is considered a subtle addition to disease susceptibility. Some known associations include ANK3 and CACNA1C (4), ODZ4 (7), BDNF (8) and DGKH (9) and others; These complex genetics slowed down research on BD, since most of the earlier research had to be done in post-mortem tissue. In this tissue, gene expression differences were found in the frontal cortex in TGF-β, Casp-8 and Tob (10). Decreased levels of the major brain antioxidant, glutathione, were found in the prefrontal cortex of patients (11). Distinct proteomic profiles of pituitary glands were reported (12). Experiments using post-mortem tissue were obviously limited. Upon the development of iPSC techniques, the study of this disease took a large step forward, enabling measurements of neurons that were derived directly from BD patients. Moreover, these neurons could be generated from patients with distinct clinical characteristics, with the limitation that these neurons did not mature in an intact brain and did not get the precise differentiation signals and cues.

The hyperexcitability phenotype of dentate gyrus (DG) hippocampal neurons derived from BD patients was first reported in our initial study (13). We replicated these findings in another cohort, showing again that DG hippocampal neurons were hyperexcitable (14). The hyperexcitability appeared in the form of sustained firing activity in high current injection. The physiology of the neurons derived from lithium-responsive (LR) patients was very different from those derived from non-responsive (NR) patients. Other studies have shown differences in the transcriptomics of neurons derived from BD patients (15) and changes in the expression of genes critical for neuroplasticity such as WNT pathway components and ion channel subunits (16). Tobe et al. (17) used proteomics profiling of human iPSCs from BD patients and showed that lithium changed the phosphorylation of CRMP2. Overall,

despite these new discoveries based on iPSC technology, the mechanisms underlying the causes of BD remain elusive, and we are still far from finding better treatment.

In this study, we used a new protocol that we recently developed (18) to search for a phenotype in CA3 pyramidal hippocampal neurons. We have found a similar phenotype of hyperexcitability in these neurons, but only in those derived from the LR patients. Delving deeper in the search for a mechanism, we observed that this hyperexcitability was correlated with the amplitude and fast kinetics of the fast potassium channels. qPCR confirmed that Kv3.1 and Kv3.2 were over-expressed in these BD LR neurons. BD NR neurons, although not significantly hyperexcitable as CA3 neurons, had drastically reduced sodium currents and increased fast potassium currents with a slower kinetics. Interestingly, a non-CNS neuron - the spinal motor neuron - did not exhibit the hyperexcitability phenotype in either BD LR or NR, further indicating that the physiological changes are neuronal type specific.

Methods

Patients

The cohort in this study consisted of the same patients used in the previous study (14). Supplementary table 1 summarizes their clinical data. The cohort consisted of 4 control individuals, 3 BD LR patients, and 3 BD NR patients. All experiments were performed on all 10 lines (Supplement).

Cell culture: DG neurons

Using iPSC technology, DG granule neurons were cultured according to our published protocol (19) and measured at t2=4.5 weeks and t1=2.5 weeks (Supplement).

Cell culture: CA3 neurons

Using iPSC technology, CA3 pyramidal neurons were cultured according to our published protocol (18) (Supplement).

For both types of hippocampal neurons, experiments were conducted at the t2 (4.5 weeks) time point, except for some of the supplemental material for which time point t1 is also shown.

Cell culture: motor neurons

Motor neurons were cultured similar to our published protocol (20) (see Supplement)

Whole cell patch clamp

Neurons were infected with the ELAVL2::eGFP lentiviral vector at 15 days differentiation. Neurons on coverslips were transferred to a recording chamber in standard recording medium containing (in mM) 10 HEPES, 4 KCl, 2 CaCl2,1 MgCl2, 139 NaCl, and 10 D-glucose (310 mOsm, pH 7.4). Whole-cell patch-clamp recordings were performed from ELAVL2::eGFP-highlighted CA3 pyramidal neurons typically at 2 recording dates: around 2.5 weeks of differentiation (t1) and at 4.5 weeks of differentiation (t2). Patch electrodes were filled with internal solutions containing (in mM) 130 K-gluconate, 6 KCl, 4 NaCl, 10

Na-HEPES, 0.2 K-EGTA, 0.3 GTP, 2 Mg-ATP, 0.2 cAMP, 10 Dglucose, 0.15% biocytin and 0.06% rhodamine. The pH and osmolarity of the internal solution were brought close to physiological conditions (pH 7.3, 290–300 mOsmol) (pipette tip resistance was typically 10–15MΩ).

Lithium treatment

Cultures of CA3 neurons were treated with 1 mM LiCl starting at 16 days of differentiation by exchanging 50% of the media daily, similar to the chronic treatment they had been exposed to in our previous study (14), Electrophysiological recordings were conducted at t2. We have recorded and analyzed a total of 56 control neurons, 49 control Li-treated neurons, 43 LR neurons, 41 LR Li-treated neurons, 71 NR neurons, and 65 NR Li-treated neurons.

Analysis of electrophysiological recordings (Supplement)

Tracing of neural progenitor cells (NPCs) (Supplement)

Channel blockers: Channel blockers were applied to the extracellular recording solution at the following concentrations: 1 mM tetraethylammonium chloride (TEA cat. 306850 R&D systems), 0.3 mM 4-aminopyridine (4-AP Tocris cat. 940100) and 200 nM α-dendrotoxin (DTX Bachem, cat. H-1088).

Immunohistochemistry (Supplement)

RNA preparation and qPCR: CA3 neurons—Total cellular RNA was extracted from 3-5 million cells per sample at 30 days post-differentiation using the RNA-BEE (QIAGEN) (Supplement).

Results

CA3 pyramidal neurons derived from BD patients are hyperexcitable only when derived from LR patients, and spike shape properties are altered

Both DG and CA3 neurons were patch clamped at time point t2 (4.5 weeks). We partitioned our data into 3 groups: neurons derived from control individuals, neurons derived from BD patients who responded to lithium (LR), and neurons derived from BD patients who did not respond to lithium (NR). Around 60% of the neurons in the 3 groups were CA3 pyramidal neurons, expressing the ELAVL2 protein (a specific CA3 protein, see Supplementary Figure 1A, 1C for immunostaining), and approximately 12% of the neurons expressed GABA (see Supplementary Fig. 1B, 1D). The total number of action potentials produced in 35 first depolarization steps (see Supplement) was counted, and this number served as the measure for excitability throughout this study. Unlike DG neurons, where both LR and NR DG neurons were hyperexcitable compared to control neurons, only LR CA3 neurons were hyperexcitable compared to control CA3 neurons (Fig. 1A for averages and Fig. 1B-D for representative recordings). This hyperexcitability of the LR CA3 neurons appeared in the form of the ability to sustain activity with high current injections (Fig. 1E-G shows representative traces with a 50 pA current injection). LR neurons recovered faster from sodium inactivation periods and were therefore able to sustain activity in high current injections. Like DG LR neurons, LR CA3 neurons also exhibited a faster rate of spontaneous

activity (Fig. 1H). The spike shape features of DG and CA3 neurons were different between the 3 groups in the recording time t2 (a time point that is slightly different than the 3.5 weeks recording time point in our previous study). The fast AHP was increased in both LR and NR DG neurons, but only in LR CA3 neurons compared to the controls (Fig. 1I-K for example recordings, and Fig. 1L for averages). (The development over time is shown in Supplementary Figure 2A for DG and CA3 neurons). The spike height was similarly larger for LR neurons both in DG and in CA3 neurons (Fig. 1M); spike width was narrowest for LR CA3 neurons (Fig. 1N). The threshold for evoking an action potential was more depolarized in NR DG neurons, with no significant changes in NR CA3 neurons (Fig. 1O). The input conductance was increased in NR CA3 neurons (Fig. 1P).

Sodium and potassium currents are altered in BD hippocampal neurons

Trying to pinpoint what the changes in the BD neurons might contribute to the hyperexcitability phenotype, we compared sodium and potassium currents between the 3 groups. Figure 2A shows a representative trace of recorded potassium currents in voltage clamp mode (Figure 2B is an expansion of the section that is between the black dotted lines of Fig. 2A). Figure 2C and 2D show the averages of the amplitude of the fast potassium currents in CA3 and DG neurons, and Fig. 2E and 2F present the averages over the slow potassium currents. Figure 2G and 2H present the amplitude of the fast potassium currents in CA3 and DG neurons at 0 mV and 20 mV depolarization potentials (respectively) for the 3 groups, which is increased in BD neurons (calculated manually, see Supplementary Methods).

The potassium currents were different not just in amplitude but also in their kinetics. The activation kinetics (see Supplementary Methods) was significantly faster in LR CA3 neurons compared to NR and control neurons, and for DG neurons it was faster in LR compared to NR neurons (Fig. 2I, 2J, for CA3, LR compared to NR $p=0.05$ ANOVA over 0-80mV range, LR compared to control $p=0.01$ over 80-90 mV range. For DG at −20 mV $p=0.03$ LR compared to NR). The inactivation kinetics in CA3 neurons was faster in LR neurons compared to NR and control neurons (in the −10-10 mV range LR to control $p=0.0038$, NR to control $p=0.01$ and $p=0.05$, LR to NR $p=0.0003$); in DG neurons, the control neurons inactivation kinetics was faster compared to NR neurons ($p=0.05$ between −20-20 mV), (Fig. 2K, 2L).

We measured sodium currents (see Supplementary Methods, Fig. 2M-O for CA3 representative traces). We compensated for transient capacitive currents (circled in black in Fig. 2P, 2Q) using an algorithm described in the Supplemental methods (leak subtraction). Fig. 2R shows the measured current in red and the current after compensating for capacitive currents in magenta. The black bar in Fig. 2Q, 2R shows the measured sodium current. Averages of the sodium currents for CA3 and DG are shown in Fig. 2S-T. It is important to note that, due to possible axonal sodium currents, the measurements can be considered accurate only in the −20 mV to 20 mV range of depolarization steps (see Supplementary for details). CA3 NR neurons had significantly lower sodium currents compared to CA3 control and CA3 LR neurons ($p=0.002$ for normalized sodium currents at −20 mV). DG NR neurons

also had lower sodium currents compared to controls (p=0.02 for sodium currents at −20 mV).

Excitability is correlated with the amplitude and kinetics of the sodium and fast potassium currents in BD hippocampal neurons, and blocking specific potassium currents diminishes the hyperexcitability phenotype

To visualize the effects of the amplitude and kinetics of the fast potassium currents, we plotted a radius of the dots as increasing with the excitability of the cell; therefore, larger dots represent more excitable cells (see Supplemental Methods for exact mathematical formula) as a function of the amplitude of the fast potassium currents on the y axis and as a function of the time constant of the decay of the fast potassium currents on the x axis for CA3 neurons (Fig. 3A) and DG neurons (Fig. 3B). The graphs show that control and LR CA3 neurons produced more action potentials than LR and control DG neurons, respectively (as seen also in Supplementary Fig. 3A). In addition, BD CA3 neurons generally had larger amplitudes of the fast potassium currents than DG neurons. Neurons with the shorter and faster time constants were more excitable and, in DG neurons, the cells that were more excitable had larger amplitudes and faster kinetics of the fast potassium currents.

To further assess the affect that alterations in currents had on neuronal excitability, we calculated correlations between excitability and amplitude of sodium and potassium currents in CA3 neurons. We plotted the excitability as a function of the amplitude of sodium currents (at −20 mV test potential) (Fig. 3C-E). As expected, all 3 groups had a positive correlation (R=0.38. p=0.003 control, R=0.36, 0=0.016 LR, and R=0.7, p=9e-11 for NR neurons). Interestingly, there was also a significant correlation between the excitability and the amplitude of the fast potassium currents (at 10 mV) in the LR CA3 neurons (Fig. 3G, R=0.31, p=0.04) and in the NR neurons (Fig. 3H R=0.36, p=0.003), but no correlation in control neurons (Fig. 3F, R=0.03. p=0.82) was observed.

Significant correlations were also calculated between excitability and kinetics of the potassium currents. The correlation between excitability and the inactivation time constant of the fast potassium currents in all 3 groups pooled together was R=−0.38, p=6e-5 (the faster the kinetics was, the more excitable the neuron was). The correlation with the kinetics of activation time constant of the potassium currents was even more significant and, pooling all groups together, it was R=−0.26 p=1.5e-6 (again the faster the kinetics, the more excitable the neuron was). In DG neurons the correlation with the inactivation constant was borderline significant, R=−0.24, p=0.05. The correlation with the activation constant was R=−0.22, p=1.5e-6.

Next, we blocked different potassium currents using 3 different channel blockers - DTX, TEA, 4A-P (see Methods)- to look for the effect on neuronal excitability. The results are depicted in Figure 3I. Potassium blockers did not reduce the excitability of control neurons, and application of DTX made the cells significantly more excitable. DTX was previously reported to increase excitability in rat neocortical pyramidal neurons (21). However, potassium channel blockers reduced excitability in both LR and NR neurons. More specifically, all of the blockers significantly reduced the hyperexcitability in LR neurons,

with TEA having the largest effect. In NR neurons, 4-AP significantly reduced the excitability.

We performed qPCR for a few types of potassium channels to look for expression differences. Kcnc1 was significantly overexpressed in LR neurons compared to control neurons (p=0.005), and an elevated level was seen in the NR neurons that did not reach statistical significance compared to controls (p=0.07, Fig. 3J). Kcnc2 was also significantly overexpressed when comparing LR and control neurons (p=0.01, Fig. 3K), and NR neurons had a significant reduction in expression compared to controls (p=0.04). No change was observed in the expression of KCNMA1 and KCNMB1 genes (Supplementary Fig. 5A, 5B). It is good to note that fast spiking interneurons also have a strong expression of Kcnc1 and Kcnc2, and the high expression level of these channels was shown (22, 23) to assist with their fast spiking abilities, helping their fast recovery from sodium inactivation, similar to the physiology we observed for LR hippocampal neurons.

Lithium increases sodium currents but reduces capacitance and the amplitude of the fast potassium currents, resulting in a reduction of hyperexcitability of neurons derived from LR BD patients

We were interested to see the effects of chronic lithium treatment on CA3 pyramidal neurons derived from BD patients and healthy subjects. We added 1 mM of LiCl to the medium 2 weeks prior to patch clamp recordings, similar to the treatment that was used in our previous study (14). Lithium was not present during patch recordings. Similar to our previous reports on DG neurons (14), lithium reduced the hyperexcitability of LR CA3 neurons. This effect was evident both in total evoked potential measurements (Fig. 4A) and spontaneous activity (Fig. 4B) and had little or no effect on the excitability of NR and control neurons. Interestingly, chronic lithium treatment reduced the capacitance of the overly large neurons to a size that was more similar to the control neurons, both in LR and NR cells (Fig. 4C). By imaging and tracing the neurons during the electrophysiological recordings, we found that this change did not come from changes to the soma size (Fig. 4D); therefore, it likely emerged from the neurites' length and arborization. We further traced the morphology of DG neurons after chronic lithium treatment over 2 weeks and found that indeed the total length of the neurites was significantly reduced after treatment in the BD groups, with a similar trend in the control neurons (Supplementary Figure 9). We therefore believe that Li treatment slows down neuritic growth thereby slowing down the increase in cell capacitance that occurs during maturation.

Looking further into spike parameters, we found that lithium treatment reduced spike height in LR neurons (Fig. 4E), did not change the fast AHP significantly in any of the groups (Fig. 4F), broadened the spike in LR neurons (Fig. 4G), and did not alter the threshold for evoking an action potential in any of the groups (Fig. 4H). An increase in the normalized sodium currents was observed in all 3 groups (using an ANOVA for depolarization potentials between −20 mV and 20 mV; p=0.0023 for control, p=0.001 for LR and p=0.0004 for NR) (Fig. 4I-K). The changes in potassium currents after lithium treatment are shown in Figure 4L-Q. Correlations between excitability and the sodium and potassium currents are further discussed in the Supplemental results and presented in Supplementary Figure 8. Since the

correlation plots indicated that the amplitude of the fast potassium currents at 0 mV step potential were more correlated with excitability in BD neurons, we plotted the changes to the fast potassium currents after lithium treatment (Fig. 4R, 4S). We observed that these currents were reduced in LR neurons after treatment (Fig. 4R), which may be a possible cause of the reduction in excitability after lithium treatment. In addition, measurements of the decay time constants of the fast potassium currents showed that they were faster in control and NR neurons after lithium treatment, indicating faster kinetics (Fig. 4S).

While our system serves as a platform for studying the physiological effects of lithium, it is important to note the possible effect of the lithium treatment itself on the patients, which may have affected the epigenetics of the patient's lymphocytes, perhaps altering the physiology of the neurons derived from the lymphoblasts. There are studies showing evidence that iPSC reprogramming generally resets the lymphocytes' epigenetic state (24, 25). We therefore believe that, after reprogramming, the cells were rejuvenated and the changes due to chronic lithium treatment likely did not remain, but it is important to keep the two possibilities in mind.

Motor neurons

Observing what seemed to be a multi-regional hyperexcitability of BD hippocampal neurons, we were interested to see whether a completely different, non-CNS neuron would show any different phenotype or physiology in BD. We differentiated our iPSCs into spinal motor neurons (see Methods). Immunostaining for islet-positive cells (examples in Fig. 5A-C) indicated similar ratios of neurons that stained positive for both islet and MAP2 compared to neurons that were positive only for MAP2 (islet+ && MAP2+)/(islet− && MAP2+) (Fig. 5D). The same measure was used to assess excitability as for the hippocampal neurons. There were no significant changes in the excitability between the 3 groups: control, LR and NR (Fig. 5E). The spike parameters that were measured in hippocampal neurons - fast AHP (Fig. 5F), spike width (Fig. 5G), threshold (Fig. 5H) and spike amplitude (Fig. 5I) - were not significantly different between the 3 groups. There were no significant changes in capacitance (Fig. 5J) or in the input conductance (Fig. 5K) between the groups. Interestingly, sodium currents were increased in the LR neurons compared to the control neurons (using an ANOVA, p=0.04, Fig. 5L), and even more increased in NR neurons (using an ANOVA, p=3e-5, Fig. 5L). There was no significant change in the slow or fast potassium currents (Fig. 5M, 5N). To summarize, despite the increase in sodium currents in BD neurons, there were no changes in the excitability of control vs. BD motor neurons.

Discussion

BD affects approximately 1.5-2% of the worldwide population putting a huge burden on the world's health and economic systems. Animal models do not fully recapitulate this disorder, either phenotypically or genetically. The introduction of iPSC technology has allowed us for the first time to study this disorder in a dynamic human model and has enabled us to define an endophenotype of this disorder in the form of DG overexcitability (13, 14). Having developed a new protocol for CA3 pyramidal neurons (18), we were interested to see if there

were any functional changes in other types of hippocampal neurons; furthermore, we were interested in looking for the mechanisms underlying the phenotype.

In this study we reveal that BD CA3 LR neurons are hyperexcitable (whereas both LR and NR BD neurons were shown to be hyperexcitable in our previous studies of DG granule neurons). This hyperexcitability correlated with the amplitude and kinetics of their potassium currents. Moreover, qPCR experiments confirmed an overexpression of the fast kinetics potassium channels Kcnc1 and Kcnc2, which are known to assist fast spiking interneurons with their fast spiking ability. Importantly, blocking these currents using different types of potassium channel blockers diminished the hyperexcitability phenotype, with the strongest effect seen using TEA.

The NR CA3 neurons did not have a significantly increased excitability compared to the controls. However, their physiology was different: they had drastically reduced sodium currents and increased fast and slow potassium currents compared to controls, but with a slower kinetics than the CA3 LR and control neurons. In the NR neurons, potassium channel blockers also reduced their excitability, with the strongest effect seen with 4-AP. Morphological analysis of BD neurons showed that, as we previously reported for DG neurons, BD neurons were larger, with NR BD neurons being the largest. Interestingly, BD NPCs were also larger. Reviewing the literature we found reports of enlarged (26-30), smaller (31), and unchanged (32) hippocampal volume in BD patients. However, brain volume was found to be affected by the number of episodes in the patients (30, 31, 33, 34). Thus, the ability to model young hippocampal neurons from BD patients allows us to observe the morphology and function of BD hippocampal neurons before disease onset or any drug treatment.

Lithium, as the first line of treatment for BD today, is known to be a mood stabilizer. Chronic lithium treatment reduced the hyperexcitability of DG LR neurons (but not of DG NR neurons) (14) and reduced the hyperexcitability of CA3 LR neurons, as we show in this study. The treatment increased the sodium currents in all 3 groups (control, LR and NR) and decreased the amplitude of the fast potassium currents in the LR group. We hypothesize that this may be the dual mechanism by which lithium acts both to reduce depression episodes in patients on one hand (the increase in sodium currents) and to reduce mania episodes in patients on the other (the decrease of the fast potassium currents whose amplitude correlates with the CA3 LR hyperexcitability). Lithium treatment also reduced cell capacitance for BD CA3 neurons and for DG neurons (14). Lithium treatment in human patients has been shown to increase hippocampal volume compared to untreated patients. However, studies showed that the decrease in hippocampal volume without treatment is due to recurrent episodes that reduce with treatment (35, 36).

To summarize, we have unraveled some of the physiological changes in BD hippocampal neurons exhibiting an endophenotype of hyperexcitability which is neuronal type specific. Many previous studies have shown that BD manifests in the hippocampus (31, 37), but other areas of the brain have also been shown to be affected (38-42), and further studies of other neuronal types should follow. The high costs of reprogramming limit the number of patients used in such studies. Here we have used a total of 10 lines: 4 controls and 6 BD patients, of

which 3 are lithium responsive, and in our previous study we used 10 more (13) lines. While iPSC-derived neurons were shown to transcriptomically resemble fetal brain tissue and are immature, being able to observe differences in these immature neurons between patients and controls shows that there is a biological disposition to psychiatric disorder (43). Never the less, follow-up studies using techniques that allow for further maturation and also mimic brain structure better, using for example organoids, would be an important step to further understand brain development in BD.

Supplementary Material

Refer to Web version on PubMed Central for supplementary material.

Acknowledgments:

This work was supported in part by the National Cancer Institute (Grant No. P30 CA014195) and the National Institutes of Health (Grant No. R01 AG05651 [to FG]) and by the National Cooperative Reprogrammed Cell Research Groups (NCRCRG) (Grant No. U19 MH106434 [to FG]). The Gage laboratory is supported in part by the Leona M. and Harry B. Helmsley Charitable Trust Grant No. 2017-PG-MED001, the JPB Foundation, Annette C. Merle-Smith, Streim Foundation, and the Robert and Mary Jane Engman Foundation. The lymphoblast samples and the clinical data were obtained with support from Canadian Institutes of Health Research Grant No. 64410 (to MA and GR). We thank Mary Lynn Gage for editing the article and we thank the Salk core facilities.

References

1. Van Meter AR, Moreira AL, Youngstrom EA (2011): Meta-analysis of epidemiologic studies of pediatric bipolar disorder. The Journal of clinical psychiatry. 72:1250–1256. [PubMed: 21672501]
2. Merikangas KR, Akiskal HS, Angst J, Greenberg PE, Hirschfeld RM, Petukhova M, et al. (2007): Lifetime and 12-month prevalence of bipolar spectrum disorder in the National Comorbidity Survey replication. Archives of general psychiatry. 64:543–552. [PubMed: 17485606]
3. Grande I, Berk M, Birmaher B, Vieta E (2016): Bipolar disorder. Lancet. 387:1561–1572. [PubMed: 26388529]
4. Ferreira MA, O'Donovan MC, Meng YA, Jones IR, Ruderfer DM, Jones L, et al. (2008): Collaborative genome-wide association analysis supports a role for ANK3 and CACNA1C in bipolar disorder. Nature genetics. 40:1056–1058. [PubMed: 18711365]
5. Gershon ES, Alliey-Rodriguez N, Liu C (2011): After GWAS: searching for genetic risk for schizophrenia and bipolar disorder. The American journal of psychiatry. 168:253–256. [PubMed: 21285144]
6. Muhleisen TW, Leber M, Schulze TG, Strohmaier J, Degenhardt F, Treutlein J, et al. (2014): Genome-wide association study reveals two new risk loci for bipolar disorder. Nature communications. 5:3339.
7. Psychiatric GCBDWG (2011): Large-scale genome-wide association analysis of bipolar disorder identifies a new susceptibility locus near ODZ4. Nature genetics. 43:977–983. [PubMed: 21926972]
8. Neves-Pereira M, Mundo E, Muglia P, King N, Macciardi F, Kennedy JL (2002): The brain-derived neurotrophic factor gene confers susceptibility to bipolar disorder: evidence from a family-based association study. American journal of human genetics. 71:651–655. [PubMed: 12161822]
9. Baum AE, Akula N, Cabanero M, Cardona I, Corona W, Klemens B, et al. (2008): A genome-wide association study implicates diacylglycerol kinase eta (DGKH) and several other genes in the etiology of bipolar disorder. Molecular psychiatry. 13:197–207. [PubMed: 17486107]
10. Bezchlibnyk YB, Wang JF, McQueen GM, Young LT (2001): Gene expression differences in bipolar disorder revealed by cDNA array analysis of post-mortem frontal cortex. Journal of neurochemistry. 79:826–834. [PubMed: 11723175]
11. Gawryluk JW, Wang JF, Andreazza AC, Shao L, Young LT (2011): Decreased levels of glutathione, the major brain antioxidant, in post-mortem prefrontal cortex from patients with

psychiatric disorders. The international journal of neuropsychopharmacology. 14:123–130. [PubMed: 20633320]

12. Stelzhammer V, Alsaif M, Chan MK, Rahmoune H, Steeb H, Guest PC, et al. (2015): Distinct proteomic profiles in post-mortem pituitary glands from bipolar disorder and major depressive disorder patients. Journal of psychiatric research. 60:40–48. [PubMed: 25455508]
13. Mertens J, Wang QW, Kim Y, Yu DX, Pham S, Yang B, et al. (2015): Differential responses to lithium in hyperexcitable neurons from patients with bipolar disorder. Nature. 527:95–99. [PubMed: 26524527]
14. Stern S, Santos R, Marchetto MC, Mendes APD, Rouleau GA, Biesmans S, et al. (2018): Neurons derived from patients with bipolar disorder divide into intrinsically different sub-populations of neurons, predicting the patients' responsiveness to lithium. Mol Psychiatry. 23:1453–1465. [PubMed: 28242870]
15. Kim KH, Liu J, Sells Galvin RJ, Dage JL, Egeland JA, Smith RC, et al. (2015): Transcriptomic Analysis of Induced Pluripotent Stem Cells Derived from Patients with Bipolar Disorder from an Old Order Amish Pedigree. PloS one. 10:e0142693. [PubMed: 26554713]
16. Madison JM, Zhou F, Nigam A, Hussain A, Barker DD, Nehme R, et al. (2015): Characterization of bipolar disorder patient-specific induced pluripotent stem cells from a family reveals neurodevelopmental and mRNA expression abnormalities. Molecular psychiatry. 20:703–717. [PubMed: 25733313]
17. Tobe BTD, Crain AM, Winquist AM, Calabrese B, Makihara H, Zhao WN, et al. (2017): Probing the lithium-response pathway in hiPSCs implicates the phosphoregulatory set-point for a cytoskeletal modulator in bipolar pathogenesis. Proceedings of the National Academy of Sciences of the United States of America. 114:E4462–E4471. [PubMed: 28500272]
18. Sarkar A, Mei A, Paquola ACM, Stern S, Bardy C, Klug JR, et al. (2018): Efficient Generation of CA3 Neurons from Human Pluripotent Stem Cells Enables Modeling of Hippocampal Connectivity In Vitro. Cell Stem Cell. 22:684–697 e689. [PubMed: 29727680]
19. Yu DX, Di Giorgio FP, Yao J, Marchetto MC, Brennand K, Wright R, et al. (2014): Modeling hippocampal neurogenesis using human pluripotent stem cells. Stem cell reports. 2:295–310. [PubMed: 24672753]
20. Marchetto MC, Muotri AR, Mu Y, Smith AM, Cezar GG, Gage FH (2008): Non-cell-autonomous effect of human SOD1 G37R astrocytes on motor neurons derived from human embryonic stem cells. Cell stem cell. 3:649–657. [PubMed: 19041781]
21. Bekkers JM, Delaney AJ (2001): Modulation of excitability by alpha-dendrotoxin-sensitive potassium channels in neocortical pyramidal neurons. J Neurosci. 21:6553–6560. [PubMed: 11517244]
22. Martina M, Schultz JH, Ehmke H, Monyer H, Jonas P (1998): Functional and molecular differences between voltage-gated K+ channels of fast-spiking interneurons and pyramidal neurons of rat hippocampus. The Journal of neuroscience : the official journal of the Society for Neuroscience. 18:8111–8125. [PubMed: 9763458]
23. Kaczmarek LK, Zhang Y (2017): Kv3 Channels: Enablers of Rapid Firing, Neurotransmitter Release, and Neuronal Endurance. Physiol Rev. 97:1431–1468. [PubMed: 28904001]
24. Mertens J, Paquola ACM, Ku M, Hatch E, Bohnke L, Ladjevardi S, et al. (2015): Directly Reprogrammed Human Neurons Retain Aging-Associated Transcriptomic Signatures and Reveal Age-Related Nucleocytoplasmic Defects. Cell Stem Cell. 17:705–718. [PubMed: 26456686]
25. Frobel J, Hemeda H, Lenz M, Abagnale G, Joussen S, Denecke B, et al. (2014): Epigenetic rejuvenation of mesenchymal stromal cells derived from induced pluripotent stem cells. Stem cell reports. 3:414–422. [PubMed: 25241740]
26. Beyer JL, Kuchibhatla M, Payne ME, Moo-Young M, Cassidy F, Macfall J, et al. (2004): Hippocampal volume measurement in older adults with bipolar disorder. Am J Geriatr Psychiatry. 12:613–620. [PubMed: 15545329]
27. Brambilla P, Harenski K, Nicoletti M, Sassi RB, Mallinger AG, Frank E, et al. (2003): MRI investigation of temporal lobe structures in bipolar patients. Journal of psychiatric research. 37:287–295. [PubMed: 12765851]

28. Strakowski SM, DelBello MP, Sax KW, Zimmerman ME, Shear PK, Hawkins JM, et al. (1999): Brain magnetic resonance imaging of structural abnormalities in bipolar disorder. Archives of general psychiatry. 56:254–260. [PubMed: 10078503]
29. Cao B, Bauer IE, Sharma AN, Mwangi B, Frazier T, Lavagnino L, et al. (2016): Reduced hippocampus volume and memory performance in bipolar disorder patients carrying the BDNF val66met met allele. Journal of affective disorders. 198:198–205. [PubMed: 27018938]
30. Javadapour A, Malhi GS, Ivanovski B, Chen X, Wen W, Sachdev P (2010): Hippocampal volumes in adults with bipolar disorder. J Neuropsychiatry Clin Neurosci. 22:55–62. [PubMed: 20160210]
31. Blumberg HP, Kaufman J, Martin A, Whiteman R, Zhang JH, Gore JC, et al. (2003): Amygdala and hippocampal volumes in adolescents and adults with bipolar disorder. Archives of general psychiatry. 60:1201–1208. [PubMed: 14662552]
32. Videbech P, Ravnkilde B (2004): Hippocampal volume and depression: a meta-analysis of MRI studies. The American journal of psychiatry. 161:1957–1966. [PubMed: 15514393]
33. Strakowski SM, DelBello MP, Zimmerman ME, Getz GE, Mills NP, Ret J, et al. (2002): Ventricular and periventricular structural volumes in first- versus multiple-episode bipolar disorder. The American journal of psychiatry. 159:1841–1847. [PubMed: 12411217]
34. Cao B, Passos IC, Mwangi B, Amaral-Silva H, Tannous J, Wu MJ, et al. (2017): Hippocampal subfield volumes in mood disorders. Molecular psychiatry. 22:1352–1358. [PubMed: 28115740]
35. Hajek T, Kopecek M, Hoschl C, Alda M (2012): Smaller hippocampal volumes in patients with bipolar disorder are masked by exposure to lithium: a meta-analysis. J Psychiatry Neurosci. 37:333–343. [PubMed: 22498078]
36. Zung S, Souza-Duran FL, Soeiro-de-Souza MG, Uchida R, Bottino CM, Busatto GF, et al. (2016): The influence of lithium on hippocampal volume in elderly bipolar patients: a study using voxel-based morphometry. Transl Psychiatry. 6:e846. [PubMed: 27351600]
37. Fatemi SH, Earle JA, McMenomy T (2000): Reduction in Reelin immunoreactivity in hippocampus of subjects with schizophrenia, bipolar disorder and major depression. Molecular psychiatry. 5:654–663, 571. [PubMed: 11126396]
38. Rajkowska G, Halaris A, Selemon LD (2001): Reductions in neuronal and glial density characterize the dorsolateral prefrontal cortex in bipolar disorder. Biological psychiatry. 49:741–752. [PubMed: 11331082]
39. Lawrence NS, Williams AM, Surguladze S, Giampietro V, Brammer MJ, Andrew C, et al. (2004): Subcortical and ventral prefrontal cortical neural responses to facial expressions distinguish patients with bipolar disorder and major depression. Biological psychiatry. 55:578–587. [PubMed: 15013826]
40. Hibar DP, Westlye LT, Doan NT, Jahanshad N, Cheung JW, Ching CRK, et al. (2018): Cortical abnormalities in bipolar disorder: an MRI analysis of 6503 individuals from the ENIGMA Bipolar Disorder Working Group. Molecular psychiatry. 23:932–942. [PubMed: 28461699]
41. Abe C, Ekman CJ, Sellgren C, Petrovic P, Ingvar M, Landen M (2015): Manic episodes are related to changes in frontal cortex: a longitudinal neuroimaging study of bipolar disorder 1. Brain : a journal of neurology. 138:3440–3448. [PubMed: 26373602]
42. Altshuler LL, Bartzokis G, Grieder T, Curran J, Mintz J (1998): Amygdala enlargement in bipolar disorder and hippocampal reduction in schizophrenia: an MRI study demonstrating neuroanatomic specificity. Archives of general psychiatry. 55:663–664. [PubMed: 9672058]
43. Brennand K, Savas JN, Kim Y, Tran N, Simone A, Hashimoto-Torii K, et al. (2015): Phenotypic differences in hiPSC NPCs derived from patients with schizophrenia. Molecular psychiatry. 20:361–368. [PubMed: 24686136]

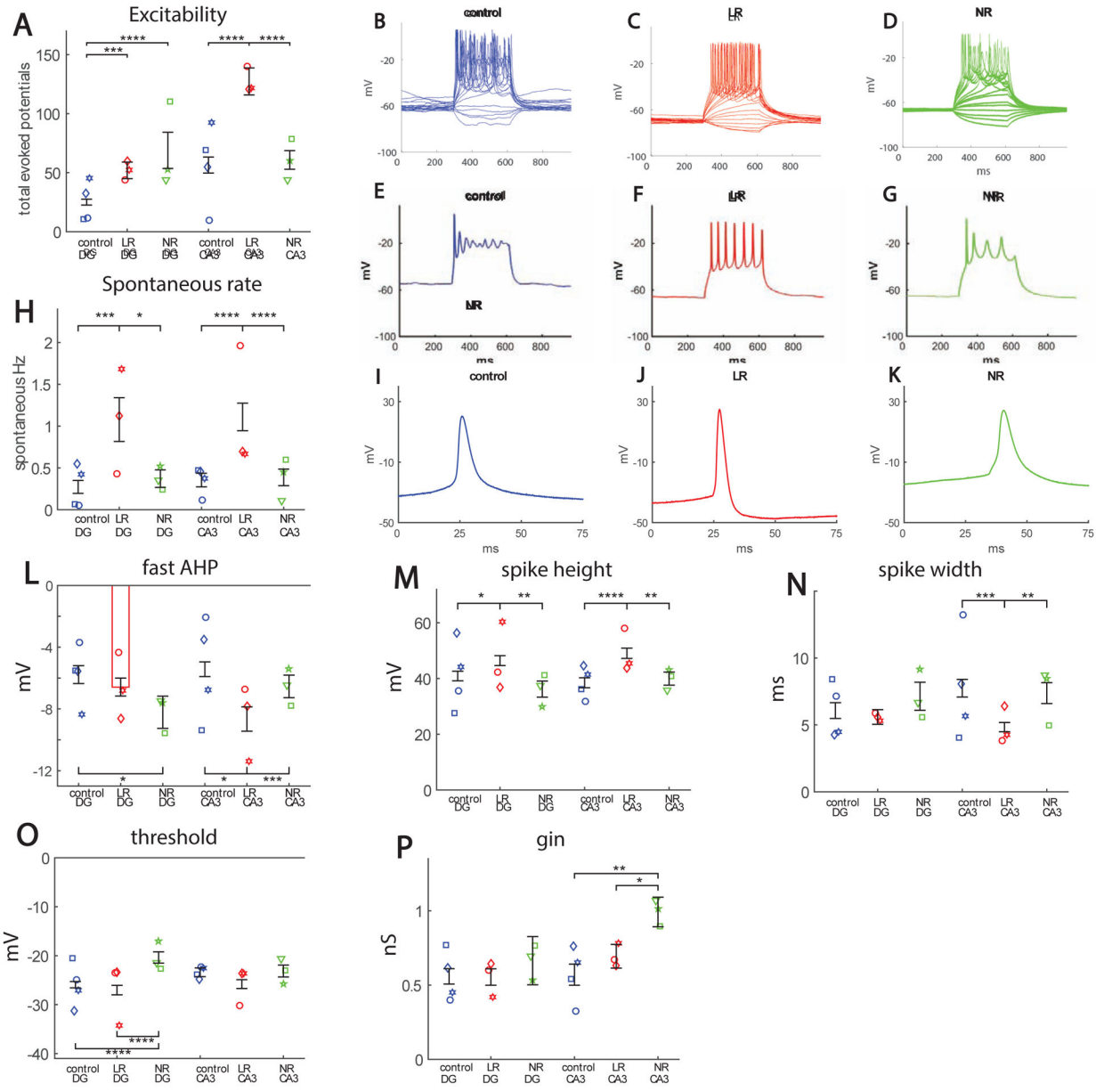

Figure 1.

Hyperexcitability in hippocampal neurons derived from BD patients. A. Cells patched at 4.5 weeks (t2) from start of differentiation. The points represent the mean of each cell line (patient), but the number of total neurons patched is as follows: DG: control 76 neurons, LR 69 neurons, NR 25 neurons; CA3: control 58 neurons, LR 46 neurons, NR 71 neurons. DG BD LR and NR neurons are hyperexcitable when compared to controls, but only BD LR CA3 neurons are hyperexcitable compared to controls. B. Representative recordings in current clamp mode of evoked potentials for a control (blue), C. LR (red) and D. NR (green) neuron. Plotting only the high current injection component reveals that the hyperexcitability of LR neurons was in the form of sustained activity with high current injections, as can be seen from the representative traces of the E. control (blue), F. LR (red) and G. NR (green) CA3 neurons. H. Spontaneous activity. BD LR neurons have an increase in the rate of

spontaneous activity both in DG and CA3 neurons. Analysis of spike shape. I. Example recordings of a single spike in current clamp mode of a control (blue) neuron, J. LR (red) neuron and K. NR (green) neuron. L. The fast after-hyperpolarization (AHP) is increased in the BD NR DG neuron at the t2 time point. Our previous report at t* (~3.5 weeks) ~ (14) showed that DG LR fast AHP was also increased at that time point. Fast AHP is also increased in BD LR CA3 neurons. M. Spike amplitude is larger for BD LR neurons, both in DG and CA3, when compared to control and NR neurons. N. Spike width is narrower in CA3 LR neurons. In (14), at the t* time point, DG LR neurons also displayed a narrower spike width. O. The threshold for eliciting an action potential is more depolarized in DG NR neurons (similar to our previous report) compared to control and BD LR neurons, but there is no significant change between the 3 groups in CA3 neurons. P. Input conductance is larger in CA3 BD NR neurons compared to control and BD LR neurons. Asterisks represent statistical significance by the following code: * p value<0.05, **p value<0.01, ***p<0.001, ****p<0.0001. Error bars represent standard error.

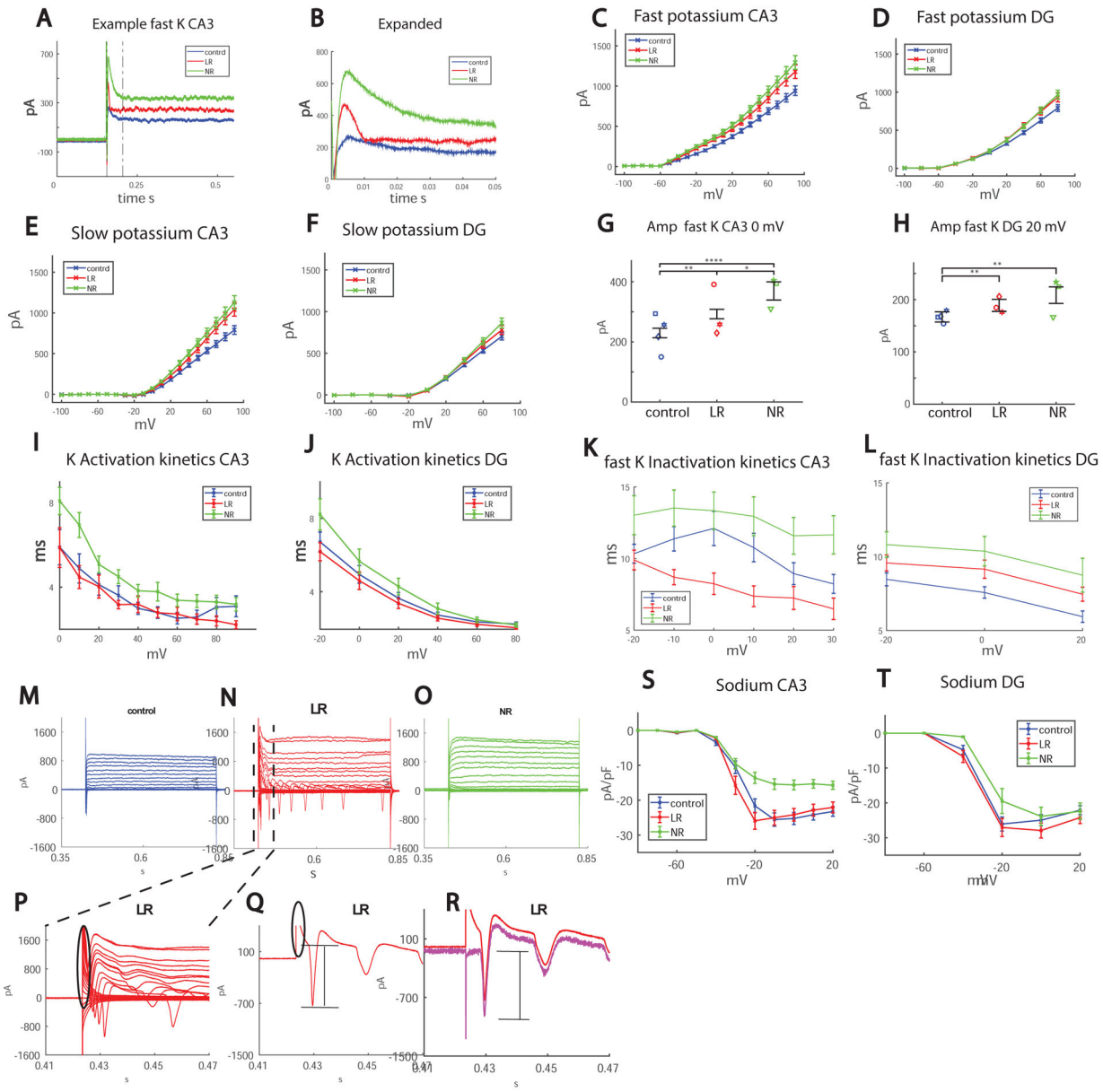

Figure 2.

Sodium and potassium currents are altered in BD hippocampal neurons. Each dot in the graphs represents an average over the total amount of patched cells for one human subject. A. Representative recordings of CA3 control (blue), LR (red) and NR (green) neurons in voltage clamp mode, displaying the increased amplitude of the fast potassium currents in BD LR and BD NR neurons and the faster inactivation kinetics in BD LR neurons. B. Expanding the area between the gray dotted lines in Fig. 2A. C. Average of fast potassium currents in CA3 neurons of the 3 groups: control, LR and NR. D. Average of fast potassium currents in DG neurons in the 3 groups: control, LR and NR. E. Average of slow potassium currents in CA3 neurons of the 3 groups: control, LR and NR. F. Average of slow potassium currents in DG neurons in the 3 groups: control, LR and NR. G-H. Manual measurements (see Supplementary Methods) were performed for the 0 mV and 20 mV test potentials, since

these were found to be the most correlated with excitability (see Fig. 3) and are inaccurate using the automatic matlab script due to fluctuations in the currents (see Supplemental Methods). G. The manual measurement of fast potassium currents in CA3 neurons at 0 mV shows a significant increase in BD LR and even more in BD NR. H. Similarly, in DG at 20 mV, BD LR neurons have increased fast potassium currents and BD NR neurons have an even more elevated level. I-J. Activation kinetics of the potassium currents. I. The activation kinetics (see Supplementary Methods) in CA3 neurons at 0-80 mV is faster in LR neurons compared to NR neurons, and faster compared to control CA3 neurons over the 80-90 mV range. J. The activation kinetics in DG neurons at −20 mV is faster in LR neurons compared to NR neurons. K-L. Fast potassium decay inactivation time. K. In LR CA3 neurons in the range of −10 mV – 10 mV (see Supplementary Methods), the decay time of the fast potassium currents is faster compared to both control and NR neurons and the control inactivation time is faster compared to NR neurons L. In DG in the −20 mV – 20mV range, NR neurons have a slower fast potassium decay time compared to control neurons. M-O. Representative recordings of the sodium currents in control (M), LR (N) and control (O) CA3 neurons. P. is an expansion of the area between the black lines of Fig. 2N. The transient capacitive currents are circled in black. Q, Same as P, but only currents due to the 10 mV depolarization step are shown. Again, the transient capacitive currents are circled in black. The sodium currents are marked with a black line and are hard to measure without compensating for the transient capacitive current. R. Using an algorithm described in the Supplementary Methods to compensate for the transient capacitive current, we calculate the sodium current that is marked with the black lines. S. Averages over the sodium currents in the 3 groups over all recordings reveal that sodium currents are reduced in NR CA3 neurons and increased in LR CA3 neurons compared to control CA3 neurons. T. Averages over the sodium currents in the 3 groups over all recordings reveal that sodium currents are reduced in NR DG neurons compared to controls.

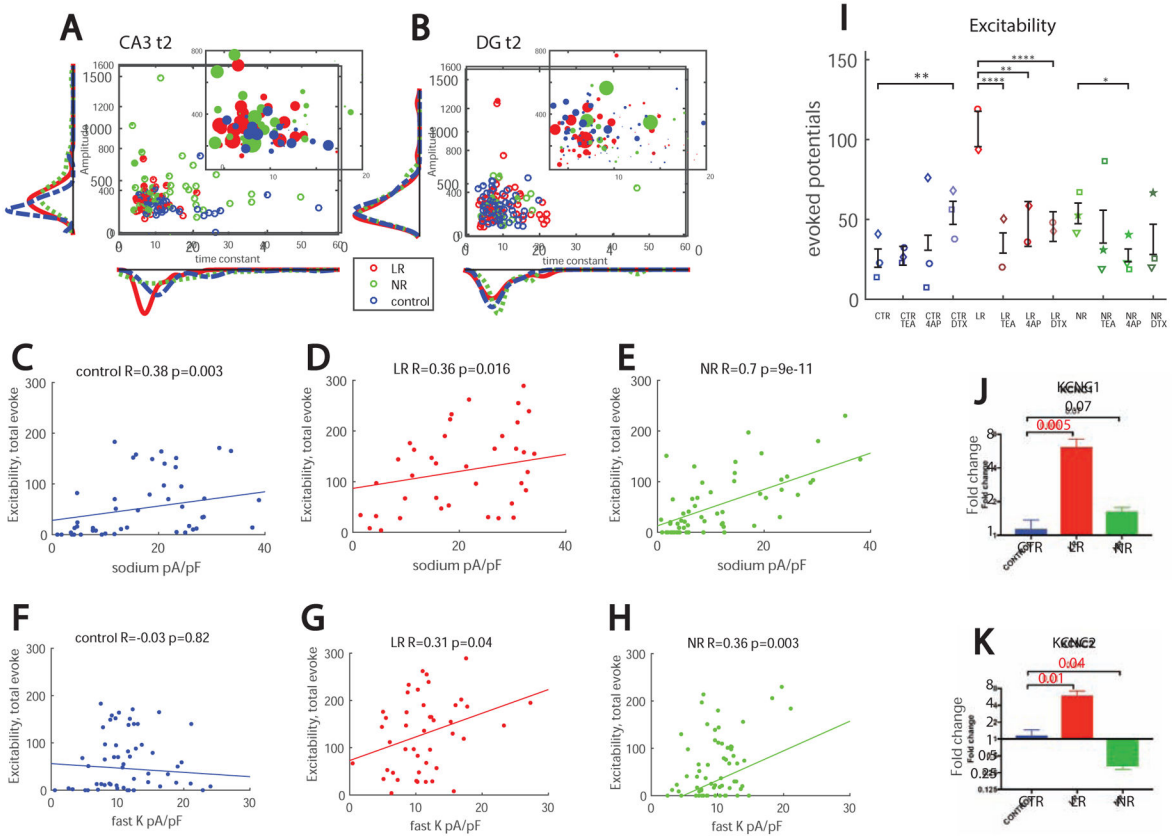

Figure 3.

Parameters affecting excitability and an overexpression of Kcnc1 and Kcnc2 in LR CA3 neurons. A.CA3 excitability (encoded in the radius of the dot, see Methods) as a function of the amplitude of the fast potassium currents (y-axis) and the kinetics or decay time constant of the fast potassium current (x-axis). The larger dots are generally observed in the neurons with fast kinetics or fast decay time of the fast potassium currents. B. DG excitability (encoded in the radius of the dot, see Methods) as a function of the amplitude of the fast potassium currents (y-axis) and the kinetics or decay time constant of the fast potassium current (x-axis). The larger dots are observed in the neurons with fast kinetics or fast decay time and higher amplitudes of the fast potassium currents. C-E. The excitability in all the groups correlates with sodium currents (at −20 mV). This correlation is much stronger in NR neurons compared to control and LR neurons. F-H. A significant correlation is observed between excitability and the amplitude of the fast potassium currents at 0 mV in LR and NR neurons. The excitability in control neurons does not correlate with the amplitude of the fast potassium currents at 0 mV. I. Blocking of different potassium channels reduced excitability of CA3 BD neurons but increased excitability of CA3 control neurons; Dendrotoxin (DTX) at 200 nM significantly increased excitability of control neurons. 1 mM Tetraethylammonium (TEA) most drastically reduced hyperexcitability of CA3 LR neurons, but 0.3 mM of 4-aminopyridine (4-AP) and DTX also significantly reduced their hyperexcitability. 4-AP reduced excitability of CA3 NR neurons. A total number of 53 control, 28 control TEA, 27 control 4-AP, 28 control DTX, 47 LR, 39 LR TEA, 18 LR 4-AP, 29 LR DTX, 104 NR, 28 NR TEA, 28 NR 4-AP and 28 NR DTX neurons were recorded. J.

qPCR results (fold change) of Kcnc1 showed that CA3 LR neurons have elevated levels compared to control neurons. K. Fold change values of Kcnc2 showed a decreased expression in NR neurons and an increased expression in LR neurons compared to CA3 control neurons. Asterisks represent statistical significance by the following code: * p value<0.05, **p value<0.01, ***p<0.001, ****p<0.0001. Error bars represent standard error.

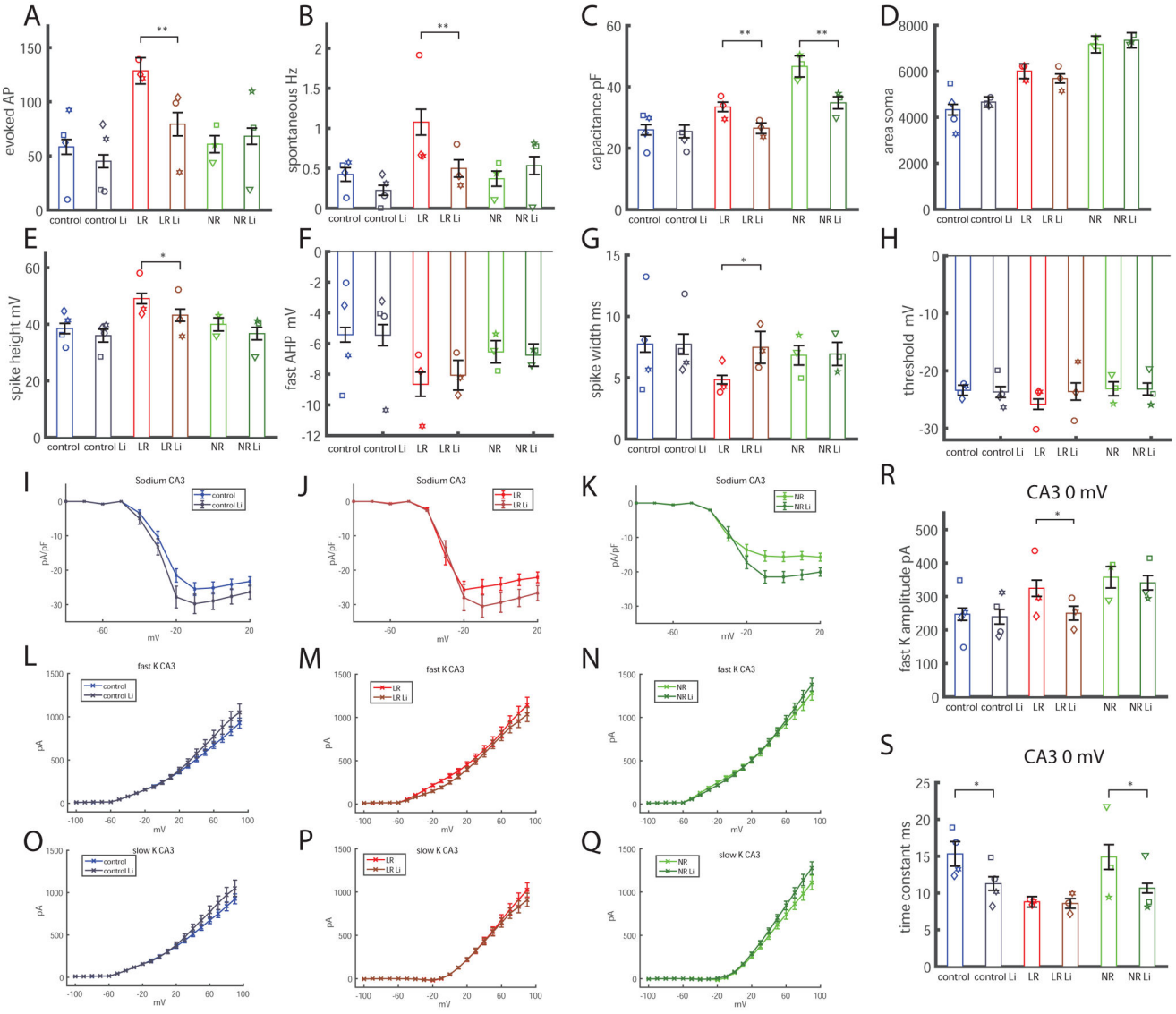

Figure 4.

Response to lithium treatment of CA3 neurons at t2. The total number of cells patched for this analysis was as follows: control, 49 neurons; control lithium (Li), 56 neurons; LR, 43 neurons; LR Li, neurons; NR, 71 neurons; NR Li, 65 neurons. A. Lithium treatment reduces the hyperexcitability (total number of evoked action potentials) of CA3 BD LR neurons. B. The spontaneous rate of action potentials is also reduced with lithium treatment in CA3 BD LR neurons. C. Similar to our previous report in DG neurons (14), the capacitance of BD LR and BD NR neurons is smaller with lithium treatment than the equivalent neurons grown without treatment. D. The soma of the BD LR and BD NR CA3 neurons did not decrease in size with lithium treatment, indicating that the reduction in capacitance with lithium treatment was due to a reduction in size of the neuritic tree. E. The spike height of BD LR CA3 neurons was reduced with lithium treatment. F. The fast AHP did not change with lithium treatment in any of the groups. G. The spike width broadened after lithium treatment in CA3 BD LR neurons. H. The threshold for evoking an action potential did not change in

any of the 3 groups following lithium treatment. I. Lithium treatment increased normalized sodium currents in control CA3 neurons. J. Lithium treatment increased normalized sodium currents in BD LR CA3 neurons. K. Lithium treatment increased normalized sodium currents in BD NR CA3 neurons. L-Q. The fast and slow potassium currents did not change significantly (ANOVA). R. The amplitude of the fast potassium current at 0 mV was significantly decreased after lithium treatment in CA3 BD LR neurons. S. The decay time constant of the fast potassium current decreased (decay was faster) with lithium treatment in CA3 control and CA3 BD NR neurons. Each dot represents an average over the total number of patched cells for one human subject. Asterisks represent statistical significance by the following code: * p value<0.05, **p value<0.01. Error bars represent standard error.

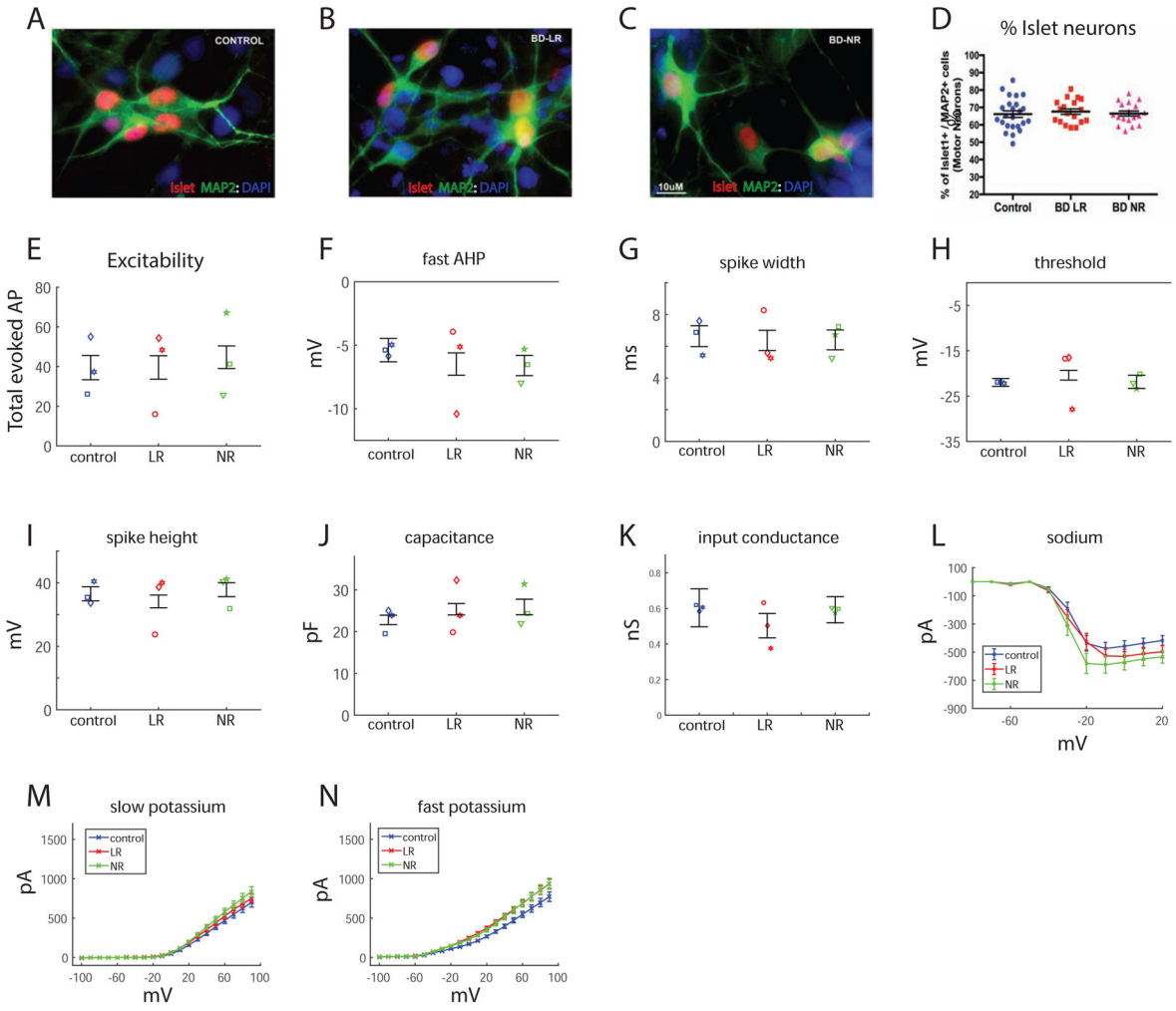

Figure 5.

Physiology of motor neurons in BD. A-D. Immunostaining for islet protein that is specific for motor neurons. A. Example image of control islet-positive neurons. B. Example image of LR islet-positive neurons. C. Example image of NR islet-positive neurons. D. Similar ratios of islet-positive neurons in the 3 groups. E. Neurons from the 3 groups display similar excitability measured by the total number of elicited action potentials. Spike parameters: fast AHP (F), spike width (G), threshold (H) and spike height (I) are similar between the 3 groups. J. Capacitance is similar between the 3 groups. K. Input conductance is similar between the 3 groups. L. Sodium currents are increased in LR and NR neurons compared to the control neurons. M. Slow potassium currents are similar between the 3 groups. N. The fast potassium current is similar between the 3 groups. Each dot represents an average over the total number of patched cells for one human subject.

KEY RESOURCES TABLE

Resource Type	Specific Reagent or Resource	Source or Reference	Identifiers	Additional Information
Add additional rows as needed for each resource type	**Include species and sex when applicable.**	**Include name of manufacturer, company, repository, individual, or research lab. Include PMID or DOI for references; use "this paper" if new.**	**Include catalog numbers, stock numbers, database IDs or accession numbers, and/or RRIDs. RRIDs are highly encouraged; search for RRIDs at https://scicrunch.org/resources.**	**Include any additional information or notes if necessary.**
Antibody	Map2ab mouse mono	Sigma		
	ELAVL2 rabbit	LSBio		
	ELAVL2/4 rabbit	LSBio		
	NeuN chicken	AveStabs		
	GABA rabbit	Sigma		
	Islet rabbit	Developmental Studies Hybridoma Bank	Cat # 39.4D5	
Bacterial or Viral Strain				
Biological Sample	human lymphoblasts	reprogrammed by Sanford Burnhem	SBP010,SBP009, SBP008, SBP011, SBP012	patietns diagnosed by Dr. Martin Alda
Cell Line				
Chemical Compound or Drug	Tetraethyl ammonium chloride, , alpha-dendroto	TOCRIS	CAS 56-34-8	
	4-aminopyriding	TOCRIS	CAS 504-24-5	
	alpha-dendrotoxin	BACHEM	H-1088.0100	
Commercial Assay Or Kit	RNA-BEE (QIAGEN)	Qiagen		
	high-capacity cDNA synthesis kit	AB Biosystems		
SYBR green	SYBR green	Life Technologies		
Deposited Data; Public Database				
Genetic Reagent				
Organism/Strain				
Peptide, Recombinant Protein				
Recombinant DNA				
Sequence-Based Reagent				
Software; Algorithm	Matlab	Mathworks	R2019	
	Clampfit	Axon pCLAMP		
	Neurolucida	mbf Bioscience		
Transfected Construct				
Other				